5938 *Inorg. Chem.* **2009**, *48*, 5938–5945
DOI: 10.1021/ic900287h

Inorganic Chemistry
Article

Electronic Structure and Magnetic Properties of Potassium Ozonide KO_3

Miquel Llunell, Pere Alemany, and Ibério de P. R. Moreira*

Departament de Química Física and Institut de Química Teòrica i Computacional (IQTCUB), Universitat de Barcelona, Martí i Franquès 1-11, 08028 Barcelona, Spain

Received February 11, 2009

The electronic structure and magnetic properties of potassium ozonide, KO_3, have been investigated by means of periodic spin polarized Hartree−Fock and Density Functional Theory based approaches. These calculations show that KO_3 is a strongly ionic compound with paramagnetic O_3^- centers. The most reliable results, provided by the B3LYP hybrid approach, suggest that the system behaves as a magnetic insulator with a gap of approximately 3.0 eV, and with the states around the insulating gap arising mainly from the π orbitals of the O_3^- units while the participation of potassium orbitals in the bands around the band gap is practically negligible. The calculations suggest that, because of the π character of the magnetic orbitals, the magnetic structure for KO_3 has a significant one-dimensional character, with antiferromagnetically coupled chains along the *c* axis and a much weaker antiferromagnetic coupling between neighboring chains. This behavior is consistent with available experimental susceptibility data.

Introduction

The magnetic properties of matter have attracted the interest of researchers since the earliest stages of modern science.[1,2] In a great number of traditional magnetic materials, like CrO_2 or NiO, the magnetic moments (which arise from the spins of unpaired electrons) are well localized on transition metal or rare-earth atoms with only a small part of the spin density transferred to other main-group atoms in the vicinity of these spin carriers. The role of these main-group atoms is, however, not negligible since in many cases they are responsible for the exchange coupling of the unpaired electrons leading to a different magnetic behavior depending on the details of this coupling.[3,4] In contrast to traditional magnetic materials, the research has focused in the last decades on molecular magnetic materials, in which the unpaired electrons are not localized on single atoms but on molecular units.[3−6] These compounds can be roughly divided in three large families. In the first one, formed by transition-metal or rare-earth compounds, the magnetic moments are still well localized on these atoms, but the exchange coupling is limited to single molecular fragments as in copper (II) acetate, where we find two copper (II) ions with their unpaired spins antiferromagnetically coupled within each $Cu_2(CH_3CO_2)_4(H_2O)_2$ molecule, but with a negligible magnetic interaction between neighboring molecules.[7] The second family comprises those materials where the spins, also mainly localized on single transition metal or rare-earth atoms, are coupled through molecular units like oxalate or cyanide anions, and not through single main-group atoms as in traditional magnetic materials. As an example of this class of compounds that have recently received considerable attention we can cite the family of Prussian-blue analogues.[8] In the third class of molecular based magnetic compounds, the unpaired electrons are no longer associated to single atoms, but to molecular units. In this category we find all organic magnets, based on organic free radicals.[5,6] Of course, it is also possible to have hybrid compounds in which we find simultaneously features of several of these three broad families in a same compound. For instance, we can couple the unpaired electrons localized on transition-metal atoms with molecular units which themselves carry unpaired electrons as in copper-(II)-nitronyl nitroxide complexes.[9,10]

In compounds of this third class, the unpaired electrons sit in molecular orbitals of the spin carrying units, and the spin density tends to be smeared out across the molecule, though

*To whom correspondence should be addressed. E-mail: i.moreira@ub.edu.

(1) Hummel, R. E. *Understanding Materials Science: History, Properties, Applications*; Springer Verlag: Heidelberg, 1998.
(2) Mattis, D. C. *The Theory of Magnetism Made Simple*; World Scientific Publishing: Singapore, 2006.
(3) Kahn, O. *Molecular Magnetism*; VCH Publishers: New York, 1993.
(4) Carlin, R. L. *Magnetochemistry*, Springer Verlag: Berlin, 1986.
(5) Miller, J. S.; Epstein, A. J. *Angew. Chem., Int. Ed. Engl.* **1994**, *33*, 385–415.
(6) Miller, J. S.; Epstein, A. J. *Chem. Commun.* **1998**, 1319–1325.
(7) Bleaney, B.; Bowers, K. D. *Proc. Roy. Soc. (London)* **1952**, *A214*, 451–465.
(8) Dunbar, K. R.; Heintz, R. A. *Prog. Inorg. Chem.* **1997**, *45*, 283–391.
(9) Caneschi, A.; Chiesi, P.; David, L.; Ferraro, F.; Gatteschi, D.; Sessoli, R. *Inorg. Chem.* **1993**, *32*, 1445–1453.
(10) Gatteschi, D.; Barra, A. L.; Caneschi, A.; Cornia, A.; Sessoli, R.; Sorace, L. *Coord. Chem. Rev.* **2006**, *250*, 1514–1529.

Published on Web 05/22/2009

normally it is concentrated on certain atoms. This situation results in a great variety of options for the topology of the exchange coupling mechanism that can lead to interesting novel magnetic properties. Although most of the materials of this type described in the literature contain organic free radicals (in most cases nitroxides) there are a few examples of simple inorganic solids with paramagnetic molecular units.[10] These compounds are especially interesting from a theoretical point of view because, although they have relatively simple crystal structures, exchange coupling between partially delocalized unpaired electrons leads to a complex electronic structure that represents a tough challenge for most of the available computational methods.

In the present work we use different first principles methods to analyze the electronic structure and magnetic behavior of KO_3, a simple inorganic ionic solid containing the paramagnetic O_3^- ozonide anion as a magnetic unit that leads to a complex three-dimensional magnetically ordered system.

Crystal Structure and Experimental Data. Alkali ozonides are oxidizing agents that contain the O_3^- radical as a constituent anion. This anion contains oxygen in an oxidation state higher than -2 that is responsible for its strong oxidizing character with potential applications in synthesis or as an in situ oxygen generator. A recent review article by Jansen and Nuss provides an excellent summary of the history, synthesis, and properties of ozonides.[11] From a theoretical point of view, a detailed investigation of the electronic structure and properties of the isolated O_3^- anion using strongly correlated wave functions was reported by Koch et al.[12] and Borowski et al.[13] Among the known ozonides, those formed with the alkaline metals are those with the simplest ordered structure with well-characterized properties, although little is known about their electronic structure. This fact was one of the motivations for the present theoretical investigation, and we choose KO_3 as a simple representative material for this family of compounds.

The crystal structure of KO_3, which is isostructural to RbO_3 and CsO_3, was first described in 1963 by Azároff and Corvin,[14] but reliable data on the geometry of the O_3^- units could not be determined until 1987 by Schnick and Jansen[15] because of its metastable character with respect to O_2 release. KO_3 crystallizes in the tetragonal $I4/mcm$ space group (No. 140) with $a = 8.6358$ Å and $c = 7.1406$ Å ($Z = 8$). A more recent determination of the crystal structure gives almost identical parameters for the structure and shows that no statistical disorder is present in this material.[16] The crystal structure can be described by an alternation of K^+ and O_3^- layers perpendicular to the c direction (Figure 1, panels a and b). Within each of these layers, the ozonide anions form a regular net in which all O_3^- units are equivalent. The three-dimensional crystal array can be rationalized as a highly distorted CsCl structure in which each O_3^- anion sits in a cube formed by eight potassium atoms, although its center of mass is displaced from the geometric center of the cube (Figure 1c).

Formally, an O_3^- anion corresponds to a 19 electrons in 10 orbitals system that leads to a local doublet state in good agreement with its behavior as an effective $S = 1/2$ magnetic particle found experimentally (see below). Each O_3^- unit in KO_3 crystal has a local C_{2v} symmetry with an O−O bonding distance of 1.346 Å and a bonding angle of 113.54°. Since the unpaired excess electron occupies an antibonding orbital, the formal bond order for O_3^- is 1.25, and hence, larger than in O_2^{2-} (1.0) and smaller than in the ozone molecule (1.5). These formal bond orders agree well with the trends observed for the O−O distances in K_2O_2 (1.541 Å),[17] KO_3 (1.346 Å) and ozone (1.272 Å).[18,19] The experimental determination of the electron density in KO_3 shows that,[16] according to the Hirshfield partitioning scheme, within the O_3^- anions, terminal O(2) atoms carry more negative partial charges (−1.0e) than the central O(1) atom (+1.2e), in line with population analyses of molecular orbitals obtained from ab initio calculations.[12] In this respect, central O(1) atoms would act as electron acceptors toward the excess electron density of terminal O(2) atoms of neighboring O_3^- units (Figure 1a). The shortest intramolecular O(1)···O(2) distance is 3.011 Å, but surprisingly the experimental study of the electron density reveals that the lone pair peaks of terminal O(2) atoms do not lie on the O(1)···O(2) line, while the lone-pair peak of O(1) does to some extent. This picture does not agree with what is expected for electrostatic dipole−dipole interactions as, for instance, in a hydrogen bond in which the lone pair of the oxygen atom (negative part of the dipole) is polarized toward the region of electron deficiency at the proton of the hydrogen bond donor. However, in the case of KO_3 the basic interactions are due to the electrostatic interactions between O_3^- and K^+ charged units that are expected to govern the final structure of the material.

The brownish-red crystals of KO_3 are paramagnetic as shown by Electron Paramagnetic Resonance (EPR)[20] and susceptibility[21] studies with magnetic moments of 1.74 μ_B obtained from a fit to the Curie−Weiss observed behavior. This value is in good agreement with the effective spin-only $S = 1/2$ moments expected for the O_3^- units. The susceptibility curve[21] shows, however, a broad maximum around 20 K and a minimum at 6 K, an indication of antiferromagnetism and three-dimensional (3D) magnetic ordering at low temperatures, that is, a complex magnetic structure with competing weak exchange couplings in different directions of the unit cell. This is also evidenced in the EPR study[20] in which the g-values are affected by exchange interactions between the O_3^- magnetic centers (for O_3^-: $g_x = 2.006$, $g_y = 2.017$, and $g_z = 2.010$). In the literature there has been, to the best of

(11) Jansen, M.; Nuss, H. *Z. Anorg. Allg. Chem.* **2007**, *633*, 1307–1315.
(12) Koch, W.; Frenking, G.; Steffen, G.; Reinen, D.; Jansen, M.; Assenmacher, W. *J. Chem. Phys.* **1993**, *99*, 1271–1277.
(13) Borowski, P.; Roos, B. O.; Racine, S. C.; Lee, T. J.; Carter, S. *J. Chem. Phys.* **1995**, *103*, 266–273.
(14) Azároff, L. V.; Corvin, I. *Proc. Nat. Acad. Sci.* **1963**, *49*, 1–5.
(15) Schnick, W.; Jansen, M. *Rev. Chim. Miner.* **1987**, *24*, 446–456.
(16) Kellersohn, T.; Korber, N.; Jansen, M. *J. Am. Chem. Soc.* **1993**, *115*, 11254–11258.
(17) Bremm, T.; Jansen, M. *Z. Anorg. Allg. Chemie* **1992**, *610*, 64–66.
(18) Tanaka, T.; Morimo, Y. *J. Mol. Spectrosc.* **1970**, *33*, 538–551.
(19) Marx, R.; Ibberson, R. M. *Solid State Sci.* **2001**, *3*, 195–202.
(20) Steffen, G.; Hesse, W.; Jansen, M.; Reinen, D. *Inorg. Chem.* **1991**, *30*, 1923–1926.
(21) Lueken, H.; Deussen, M.; Jansen, M.; Hesse, W.; Schnick, W. *Z. Anorg. Allg. Chem.* **1987**, *553*, 179–186.

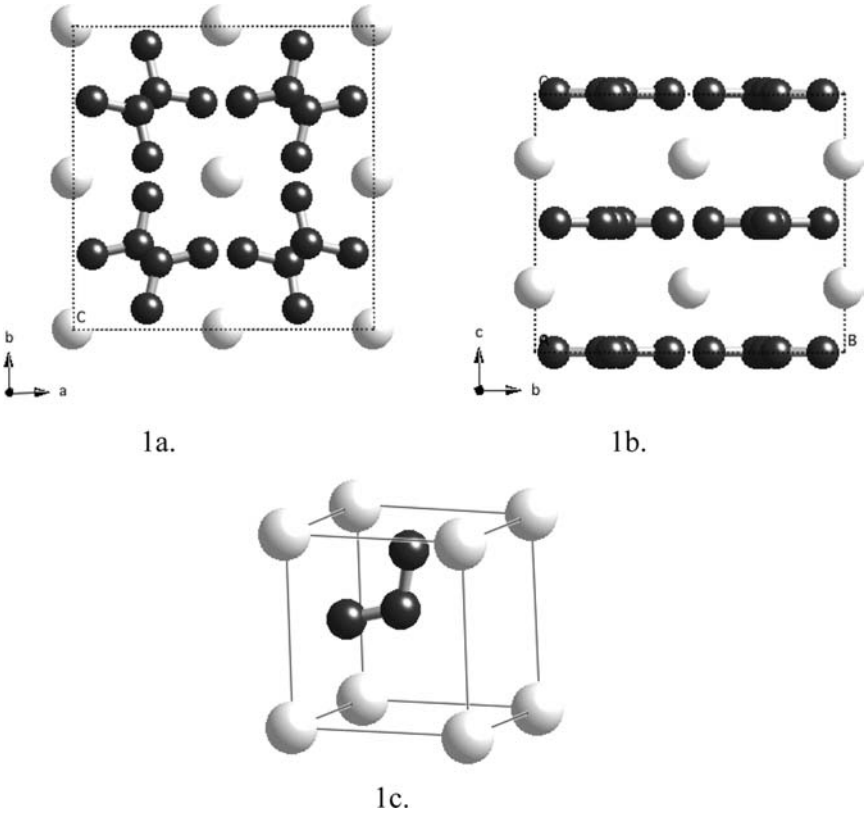

Figure 1. Details of the conventional cell of KO_3. Notice the regular net in *ab* planes formed by planar O_3^- units (Figure 1a), the distribution of these planes along *c* direction (Figure 1b), as well as the CsCl-type structure formed by each KO_3 unit (Figure 1c). Dark connected spheres correspond to oxygen atoms, white large spheres to potassium atoms.

our knowledge, no attempt to estimate the dominant magnetic interactions for this compound.

Computational Details

The computational study of the electronic structure and the magnetic exchange interactions in KO_3 has been performed using the Hartree−Fock (HF) and Density Functional Theory (DFT) based methods for periodic systems as implemented in the CRYSTAL03 program.[22] A detailed description of the mathematical formulation and the algorithms in CRYSTAL has been previously published[23−26] and will be omitted here. All-electron atomic basis sets of Gaussian functions optimized for the ionic environment (86−511G basis set for K^+ (with 3sp and 4sp exponents of 0.498 and 0.169, respectively[27]) and 8−411-d (with 3sp, 4sp and d exponents of 0.45, 0.18, and 0.75, respectively[28]) for O^{2-}) have been used to describe the electron density within the LCAO approximation. To compute the relative energies of the several states arising from different arrangements of the spins for the unpaired electrons of the O_3^- anions, unrestricted (spin-polarized) HF, and DFT methods (using the hybrid B3LYP[29] and the GGA-type PBE[30] and PW91[31] functionals) have been used to obtain broken symmetry solutions within the supercell approach[32−36] (see below for more details).

For the calculation of Coulomb and exchange integrals, tolerance factors[37,38] of 7, 7, 7, 7, and 14 have been adopted to ensure enough accuracy to calculate energy differences smaller than 10^{-6} Hartree. Integration of k-dependent magnitudes has been carried out using a mesh of 300 *k*-points in the first Brillouin zone (chosen according to the Monkhorst−Pack

(22) Saunders, V. R.; Dovesi, R.; Roetti, C.; Orlando, R.; Zicovich-Wilson, C. M.; Harrison, N. M.; Doll, K.; Civalleri, B.; Bush, I.; D'Arco, Ph.; Llunell, M. *CRYSTAL2003 User's Manual*; University of Torino: Torino, Italy, 2003.
(23) Pisani, C.; Dovesi, R.; Roetti, C. Hartree-Fock ab initio treatment of crystalline systems. In *Lecture Notes in Chemistry*; Springer Verlag: Heidelberg, 1988; Vol. 48.
(24) Quantum-Mechanical ab initio calculation of the properties of crystalline materials. In *Lecture Notes in Chemistry*; C. Pisani, Ed.; Springer Verlag: Berlin, 1996; Vol. 67.
(25) Dovesi, R.; Orlando, R.; Roetti, C.; Pisani, C.; Saunders, V. R. *Phys. Status Solidi B* **2000**, *217*, 63–88.
(26) Towler, M. D.; Zupan, A.; Causa, M. *Comput. Phys. Commun.* **1996**, *98*, 181–205.
(27) Dovesi, R.; Roetti, C.; Freyria-Fava, C.; Prencipe, M.; Saunders, V. R. *Chem. Phys.* **1991**, *156*, 11–19.
(28) Towler, M. D.; Allan, N. L.; Harrison, N. M.; Saunders, V. R.; Mackrodt, W. C.; Apra, E. *Phys. Rev. B* **1994**, *50*, 5041–5054.
(29) (a) Becke, A. D. *J. Chem. Phys.* **1993**, *98*, 5648. (b) Lee, C.; Yang, W.; Parr, R. G. *Phys. Rev. B* **1988**, *37*, 785–789.
(30) Perdew, J. P.; Burke, K.; Ernzerhof, M. *Phys. Rev. Lett.* **1996**, *77*, 3865–3868.
(31) (a) Perdew, J. P.; Wang, Y. *Phys. Rev. B* **1986**, *33*, 8800–8802. (b) see also erratum in: *Phys. Rev. B* **1989**, *40*, 3399. (c) Perdew, J. P.; Wang, Y. *Phys. Rev. B* **1992**, *45*, 13244–13249.
(32) (a) Ricart, J. M.; Dovesi, R.; Roetti, C.; Saunders, V. R. *Phys. Rev. B* **1995**, *52*, 2381–2389. (b) see also erratum in: *Phys. Rev. B* **1997**, *55*, 15942-15942.
(33) Dovesi, R.; Ricart, J. M.; Saunders, V. R.; Orlando, R. *J. Phys.: Condens. Matter* **1995**, *7*, 7997–8007.
(34) Reinhardt, P.; Moreira, I. de P. R.; de Graaf, C.; Illas, F.; Dovesi, R. *Chem. Phys. Lett.* **2000**, *319*, 625–630.
(35) Moreira, I. de P. R.; Dovesi, R.; Roetti, C.; Saunders, V. R.; Orlando, R. *Phys. Rev. B* **2000**, *62*, 7816–7823.
(36) Ruiz, E.; Llunell, M.; Alemany, P. *J. Solid State Chem.* **2003**, *176*, 400–411.
(37) Dovesi, R.; Pisani, C.; Roetti, C.; Saunders, V. R. *Phys. Rev. B* **1983**, *28*, 5781–5792.
(38) Saunders, V. R.; Freyria-Fava, C.; Dovesi, R.; Salasco, L.; Roetti, C. *Mol. Phys.* **1992**, *77*, 629–665.

scheme[39] with a shrinking factor of 8 and 2 symmetry operators).

Results and Discussion

Stability of Metallic versus Insulating Magnetic Solutions. The first set of calculations is aimed toward the computation of the relative stability of the metallic (closed shell) state, obtained by forcing the pairing of all electrons in the cell, with respect to the insulating magnetic (open shell) states with one unpaired electron localized on each O_3^- unit, obtained using the spin unrestricted approaches. For this purpose we have chosen the simplest magnetic solution, that is, the ferromagnetic one, in which the four unpaired electrons in each primitive unit cell have all their spins aligned in the same direction. The calculations confirm the expected result (the solid is paramagnetic at room temperature) and the metallic phase is clearly less stable than the magnetic insulator one. The calculated energy differences per formula unit are 3.4, 0.9, 0.3, and 0.3 eV at the spin unrestricted HF, B3LYP, PBE, and PW91 levels, respectively. All four methods show without any doubt that the system behaves as a magnetic insulator, and the differences in the calculated values are just another confirmation of the typical trends in the localization-delocalization behavior exhibited by each method.[40−42] We rely on the B3LYP result as the most balanced description based on previous discussions on molecular solids[43−47] and on transition metal magnetic insulators.[36,40−42,48,49] According to our B3LYP calculations, KO_3 behaves as a magnetic insulator with a band gap of approximately 2.9 eV (0.107 au), a value that should only be considered qualitatively because of the well-known failures of DFT methods to give accurate values for this magnitude in magnetic oxides, although it is expected that B3LYP provides reasonable estimates of the spin localization and magnitude of the insulating gap. This is clearly seen in Figure 2 in which the Density of States (DOS) plots are reported. The UHF method results in a large overestimation of the insulating gap of 0.415 au (or 11.3 eV), whereas GGA methods provide values close to 0.035 au (or 1.0 eV), in line with the previous works on transition metal magnetic insulators mentioned above.

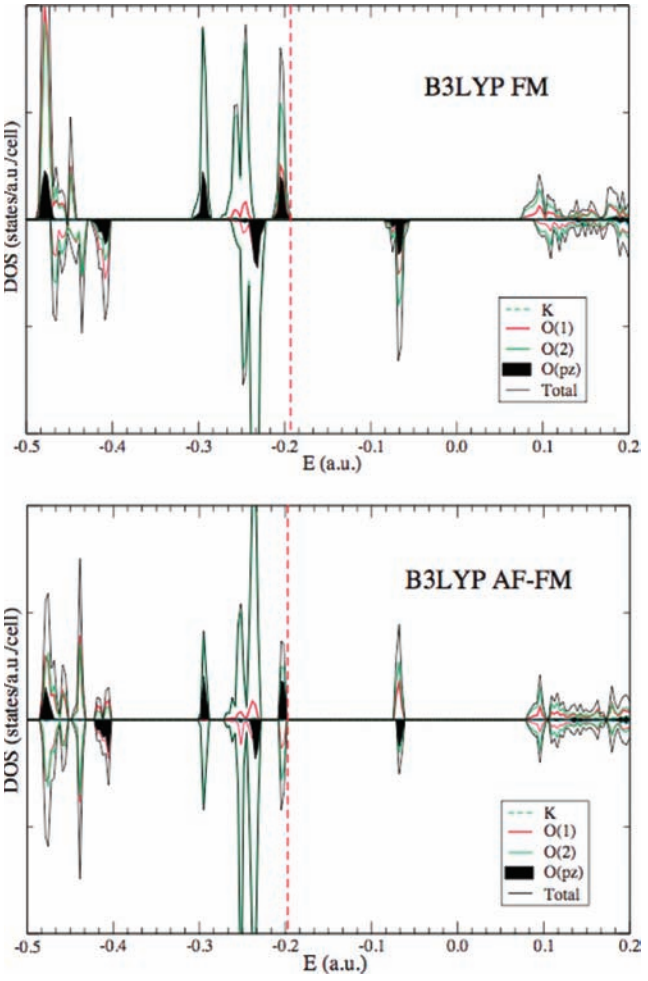

Figure 2. Total and projected DOS of the ferromagnetic and AF-FM ground state phases of KO_3 using the B3LYP approach. Notice that the projected states of K are not significant in this energy range.

It is also observed that bands with O p_z character dominate the insulating gap whereas K core and valence states appear well below and above the Fermi level, with almost no interaction with O states. This fact further corroborates the ionic character of this material suggested by the Mulliken analysis discussed below although the interaction between O_3^- units along c axis may be relevant because of the large delocalization of their π system.

Electron Density and Population Analysis. For the ferromagnetic solution, the Mulliken population analysis (Table 1) shows that KO_3 has a strongly ionic character, with the calculated charges for the K^+ cations and O_3^- anions close to +1 and −1, respectively. Although charges obtained from a Mulliken analysis should be taken cautiously, and only for qualitative purposes, it is interesting to remark that results obtained using the four different methods are very similar. The well-known trend of stronger charge localization in the UHF solution as compared to the DFT ones is present in our calculations (see the discussion above), but this different behavior is not very noticeable in the population analysis for KO_3. Our calculated charges or the O_3^- units agree well with the analysis of the experimental charge density given by

(39) Monkhorst, H. J.; Pack, J. D. *Phys. Rev.* **1976**, *13*, 5188–5192.
(40) Muscat, J.; Wander, A.; Harrison, N. M. *Chem. Phys. Lett.* **2001**, *342*, 397–401.
(41) Mallia, G.; Orlando, R.; Llunell, M.; Dovesi, R. In *Computational Materials Science*; Catlow, C. R. A., Kotomin, E. A., Eds.; IOS Press: Amsterdam, The Netherlands, 2003; pp 102−121.
(42) Cora, F.; Alfredsson, M.; Mallia, G.; Middlemiss, D. S.; Mackrodt, W. C.; Dovesi, R.; Orlando, R. In *Principles and Applications of Density Functional Theory in Inorganic Chemistry, Structure and Bonding*; McGrady, J., Kaltsoyannis, N., Eds.; Springer Verlag: Heidelberg, 2004; Vol. 113, pp 171−232.
(43) Ruiz, E.; Alemany, P.; Alvarez, S.; Cano, J. *J. Am. Chem. Soc.* **1997**, *119*, 1297–1303.
(44) Ruiz, E.; Cano, J.; Alvarez, S.; Alemany, P. *J. Am. Chem. Soc.* **1998**, *120*, 11122–11129.
(45) Ruiz, E.; Cano, J.; Alvarez, S.; Alemany, P. *J. Comput. Chem.* **1999**, *20*, 1391–1400.
(46) Ruiz, E.; Álvarez, S.; Rodríguez-Fortea, A.; Alemany, P.; Pouillon, Y.; Massobrio, C. *Electronic Structure and Magnetic Behavior in Polynuclear Transition-Metal Compounds in Magnetoscience: From Molecules to Materials*; Drillon, M., Ed.; Wiley-VCH: Weinheim, 2001; Vol. 2, pp 227−279.
(47) Ruiz, E.; Rodríguez-Fortea, A.; Cano, J.; Álvarez, S.; Alemany, P. *J. Comput. Chem.* **2003**, *24*, 982–989.
(48) Moreira, I. de P. R.; Illas, F.; Martin, R. L. *Phys. Rev. B* **2002**, *65*, 155102-(1-14).
(49) Moreira, I. de P. R.; Dovesi, R. *Int. J. Quantum Chem.* **2004**, *99*, 805–823.

Table 1. Atomic Charges and Spin Densities (in Electrons) Obtained from a Mulliken Population Analysis for the Insulating Ferromagnetic Solution for KO_3 using Different Methods[50]

atom	UHF	B3LYP	PBE	PW91
		Charge[a]		
K	0.97	0.95	0.94	0.94
O(1)	0.24	0.15	0.14	0.14
O(2)	−0.61	−0.55	−0.55	−0.55
		Spin		
K	0.00	0.00	0.00	0.00
O(1)	0.70	0.40	0.38	0.36
O(2)	0.15	0.30	0.31	0.32

[a] Because the values calculated for the two distinct K atoms in the structure are practically identical, average charges for these atoms are given as a single entry in the table.

Kellerson et al.[16] in which the terminal O(2) oxygen atoms carry a more negative partial charge than the central O(1) one. The difference between the partial charges on O(2) and O(1) that we find in our calculations is, however, much smaller (between 0.85 and 0.7e, depending on the method; see Table 1) than that found from the Hirshfeld analysis of the experimental electron density (2.2e). This value is in our opinion too large (if the four electrons in the π-system were totally localized on the terminal O(2) atoms, a maximal difference of 2.0e between the charges on O(2) and O(1) would be expected), possibly because of an artifact introduced by the numerical analysis of the experimental data, while the results obtained from quantum mechanical calculations seem to be more reasonable.

The population analysis shows also clearly that one unpaired electron is localized on each O_3^- anion. As expected from the composition of the $2b_1$ singly occupied molecular orbital (SOMO) for these anions, the spin density is larger on the central O(1) atom. In contrast with the figures obtained for the charge distribution, the UHF method is found in this case to strongly exaggerate this uneven distribution, practically localizing the unpaired electron on the central oxygen atom of each ozonide anion. Spin density values obtained from molecular electronic structure calculations on the isolated O_3^- anion[50] suggest that the spin distribution found by B3LYP is expected to provide the most reliable description of the solid.

Figure 3 shows the charge and spin density maps calculated for the ferromagnetic phase of KO_3 at the B3LYP level in a (001) plane containing the O_3^- anions (top of Figure) and several (*mn*0) planes bisecting one of the O_3^- fragments (Figures 3A, 3B and 3C). It is seen that the K^+ ions exhibit a very small charge deformation, in agreement with the strong ionicity found in KO_3. In addition, the spin density maps clearly show that the unpaired electrons are located on the π system of each O_3^- unit.

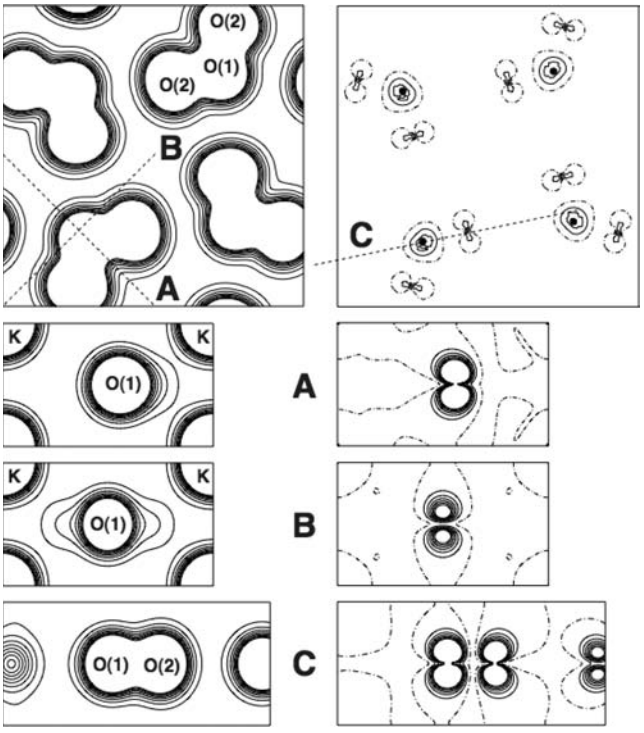

Figure 3. Total electron density (left) and spin density maps (right) in a (001) plane (top) through the O_3^- ions, and several perpendicular planes (A, B, and C) bisecting through the O_3^- units in the FM magnetic phase. For electron density maps (i.e., $\rho(\alpha)+\rho(\beta)$) the separation between contiguous isodensity curves is 0.01 |e| a_0^{-3} and the function is truncated in the atomic regions at 0.08 |e| a_0^{-3}. For spin density maps (i.e., $\rho(\alpha)-\rho(\beta)$) the separation between contiguous isodensity curves is 0.005 |e| a_0^{-3} and the most internal curves in the core regions correspond to ± 0.03 |e| a_0^{-3}. Continuous, dashed and dot-dashed lines correspond to positive (α density), negative (β density), and zero values of the function, respectively.

Electronic Structure: DOS. For all methods used in this work, the DOS plots (Figure 2) show clearly that for the ferromagnetic solution the states around the insulating gap arise mainly from the π orbitals of the O_3^- units. Both the magnitude of the gap and the nature of the bands near the Fermi level are similar either for the ferromagnetic solution (Figure 2 left) or for the ground state (with both ferro and antiferromagnetic interactions between neighboring O_3^- units, see discussion below for more details). In agreement with the results found from the population analysis that indicate a strongly ionic character for this solid, the participation of potassium orbitals in the bands around the band gap is negligible. Although the gross features of the DOS and its projections are very similar for the four methods used to obtain the electronic structure of KO_3, as expected from previous experience, the details strongly depend on the functional.[36,40−45,48,49]

Magnetic Exchange Interactions. The results discussed in the sections above clearly show that KO_3 behaves as a magnetic insulator with local $S = 1/2$ effective O_3^- spin particles that interact with their nearest neighbors through different exchange coupling paths. The strongly ionic nature of the solid, with negligible participation of K orbitals in the occupied valence bands, allows us to predict direct, through space, and hence, relatively weak exchange interactions for this compound, in good

(50) CASSCF(13,9) calculations on the isolated O_3^- anion using the same structure as in the crystal and 6-31+G* basis set provide spin population values of 0.50 and 0.25 unpaired electrons on O(1) and O(2), respectively. Interestingly enough, (spin unrestricted) B3LYP calculations on this molecular unit provide spin population values of 0.36 and 0.32 unpaired electrons on O(1) and O(2), respectively, whereas UHF provide spin population values of 0.62 and 0.19 unpaired electrons on O(1) and O(2). The total Mulliken charges for O(1) and O(2) from these molecular calculations are 0.12 and −0.55 electrons for CASSCF(13,9), 0.02 and −0.51 electrons for B3LYP, and 0.14 and −0.57 electrons for UHF.

agreement with the experimental data that show deviations of the Curie−Weiss law only at temperatures below 20 K. Since this experimentally observed behavior points to a complex magnetic structure with competing exchange coupling interactions in various directions of the unit cell, we have undertaken a series of calculations to analyze this magnetic structure.

The description of exchange coupling in a broad class of compounds including organic biradicals, polynuclear transition-metal complexes, and ionic solids is based on the use of the well-known Heisenberg−Dirac−van Vleck Hamiltonian (HDVV) in which the isotropic interaction between localized magnetic moments S_i and S_j is described by

$$H^{\mathrm{HDVV}} = -\sum_{i,j} J_{ij} \vec{S_i} \cdot \vec{S_j} \qquad (1)$$

where J_{ij} are the exchange coupling constants between S_i and S_j that give the magnitude and the nature (ferromagnetic for $J_{ij} > 0$ and antiferromagnetic for $J_{ij} < 0$) of the interaction. For the simplest case, a finite system with a pair of paramagnetic centers with effective spins S_1 and S_2 (where $S_2 \leq S_1$), respectively, the difference between the ferromagnetic (parallel) and the antiferromagnetic (antiparallel) spin configurations can be related by a simple expression involving the exchange coupling constant:

$$E_{\mathrm{AF}} - E_{\mathrm{FM}} = 2S_1S_2J_{12} \qquad (2a)$$

The use of this expression is equivalent to that obtained using the Ising Hamiltonian, which considers the S_z component of the total spin operator, to map the energy of the different magnetic solutions to the magnetic coupling constant J_{12} and has been shown to rely on well established relations between spin symmetry of the Heisenberg Hamiltonian and the space and spin broken symmetry solutions used to represent the magnetic phases.[51−53] Empirically it has been found, however, that when using DFT based methods a better numerical approximation for the coupling constant can be obtained if the spin projection procedure used to deduce the equation above is not applied. This leads to an alternative expression,[36,45−47]

$$E_{\mathrm{AF}} - E_{\mathrm{FM}} \approx 2(S_1S_2 + S_2)J_{12} \qquad (2b)$$

that for systems with $S = 1/2$ leads to one-half of the values obtained from the previous scheme. The coupling constants discussed in the following have been obtained using either the UHF method and eq 2a or the (spin unrestricted) B3LYP method and eq 2b and, in this case, only differ by a factor 2. For a detailed discussion of the calculation of exchange coupling constants using first principles methods and the approximations employed in each case, the interested reader is referred to the extensive literature on this topic.[36,45−47,51−53]

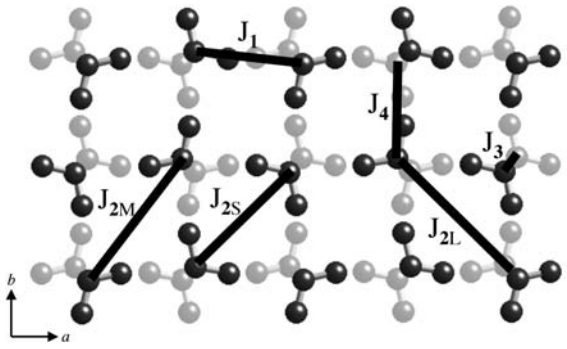

Figure 4. Representation of the pairs of O_3^- anions considered in the definition of J_1 to J_4 (two *ab* planes are shown, deepness represented by light gray tones). The different *ab* in-plane interactions are J_1 and J_2 whereas the interplane interactions along the *c* direction correspond to J_3 and J_4. Notice that actually the calculated value of J_2 corresponds to the average magnetic coupling given by J_{2L}, J_{2S}, and J_{2M}. The magnetic cells considered for the calculation of the magnetic coupling constants contain 16 O_3^- units and are obtained by doubling the conventional cell along the *c* axis.

The actual expression of the HDVV Hamiltonian for a crystal (eq 1) is, however, simplified by the following considerations: (a) the periodicity of the crystal structure allows us to restrict ourselves to interactions within a single unit cell, (b) additional symmetry elements in the crystal structure reduce the number of distinct coupling constants, and (c) in most cases, considering that the exchange interaction is limited only to nearest neighbors in the unit cell, is an excellent approximation. Taking into account these three constraints, the final goal is to determine the finite set of n coupling constants $\{J_{ij}\}$ defining the magnetic Hamiltonian that characterizes the magnetic ordering of the system and permits one to describe the lowest part of its excitation spectrum. From a computational point of view, the procedure used usually to obtain the set of coupling constants defining the HDVV Hamiltonian for a magnetic crystal consists in the calculation of $n + 1$ energies corresponding to different spin distributions within the unit cell (or within an adequate supercell if needed). Since for each pair of paramagnetic centers the energy difference between the ferromagnetic and the antiferromagnetic spin configurations is given by eq 2a or, alternatively by eq 2b, we can extend that approach to periodic extended compounds by just expressing the difference in energy between different spin configurations as a sum of pairwise interactions within the unit cell. Considering energy differences between the $n + 1$ calculated energies we can construct a system of n (independent) equations with n unknowns, the J_{ij} values. If additional magnetic phases can be calculated, a root-mean-square fit of the J_{ij} parameters to reproduce the energy of the $m > n + 1$ solutions is used. A detailed description of the procedure with some worked out examples can be found in refs 34, 35, 46, 47, and 53 and has been used in the present work. For the analysis of the magnetic structure of KO_3 we have considered the four different interaction pathways shown in Figure 4.

If we describe the crystal structure of KO_3 as a stapling of consecutive O_3^- layers $\cdots$ABABA$\cdots$ along the *c* axis, J_1 (Figure 4) is the exchange coupling constant describing the interaction between two neighboring O_3^- within one of these layers (shortest O(1)$\cdots$O(2) distance $d_1 = 3.011$ Å).

(51) Caballol, R.; Castell, O.; Illas, F.; Malrieu, J.-P.; Moreira, I. de P. R. *J. Phys. Chem. A.* **1997**, *101*, 7860–7866.
(52) Moreira, I. de P. R.; Illas, F. *Phys. Chem. Chem. Phys.* **2006**, *8*, 1645–1659.
(53) Moreira, I. de P. R.; Calzado, C. J.; Malrieu, J.-P.; Illas, F. *New J. Phys.* **2007**, *9*, 369-(1-25).

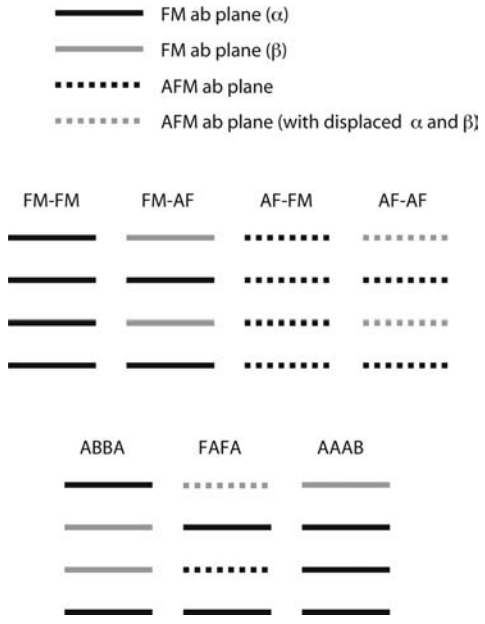

Figure 5. Schematic representation of the magnetic solutions used to calculate the values of J_1, J_2, J_3, and J_4. The labels adopted for the magnetic solutions indicate the nature of the interaction within the *ab* planes and along the perpendicular *c* axis (e.g.: the AF-FM solution contains antiferromagnetic *ab* planes coupled ferromagnetically along the *c* axis). The five additional magnetic solutions considered for completeness with $S_z = 4$ (FAFA, AAAB, and AFM1) and $S_z = 0$ (ABBA and AFM2) are more complex and are named differently. Notice that black and gray bars denote different setting of spins along *c* axis. AFM1 and AFM2 solutions (not shown) correspond to different orderings of ferromagnetic chains along *c* direction per cell, one α and three *β* chains for AFM1 and two α and two *β* for AFM2. Alternatively, the AFM2 solution can be viewed as ferromagnetically ordered *ac* (or *bc*) planes alternating its spin along the *b* (or *a*) direction.

The two coupling constants J_3 and J_4 (Figure 4, left side) describe the interactions of molecules sitting in consecutive A and B layers (the shortest O(1)···O(1) contact for J_3 is $d_3 = 3.684$ Å and the shortest O(2)···O(2) contact for J_4 is $d_4 = 3.752$ Å). Finally, we have also considered J_2 (Figure 4, right side), describing the average interaction between O_3^- units sitting in a given *ab* layer through the diagonal paths of this net (considering only O(1)···O(1) distances, there are regular plaquettes with two equivalent O(1)···O(1) distances defined by $d_{2M} = 6.152$ Å and irregular plaquettes defined by $d_{2S} = 5.357$ Å and $d_{2L} = 6.856$ Å O(1)···O(1) distances). The remaining interactions should, a priori, be much weaker than the previous ones according to the long distance between the two spin carrying units leading to too small overlap between magnetic orbitals localized on the O_3^- units.

To obtain the values for J_1 to J_4 we have considered several magnetic phases that have been constructed by starting from different localized spins on O(1) as the guess densities for the self-consistent field (SCF) procedure. The relaxed densities show spin densities localized on the O_3^- units following the patterns defined in the corresponding SCF guesses as shown in Figure 5. The labels adopted for the magnetic solutions indicate the nature of the interaction within the *ab* planes and along the perpendicular *c* axis. In the AF-FM solution, for instance, antiferromagnetic *ab* planes are coupled ferromagnetically along the *c* axis. Finally, five additional magnetic solutions with $S_z = 4$ (FAFA, AAAB, and AFM1) and $S_z = 0$ (ABBA and AFM2) have been considered together with the $S_z = 8$ (FM) and $S_z = 0$ (AF-FM, FM-AF, and AF-AF) set of solutions. Notice that these values of S_z correspond to 16, 8, and 0 unpaired electrons per magnetic cell. See Figure 5 for a simplified representation of all these magnetic solutions and Table 2 for their relative energies and corresponding energy expressions in terms of J_1, J_2, J_3 and J_4. These relations, allow us to extract the values for the coupling constants shown in Table 3 by a root-mean-square fit of J_1, J_2, J_3, and J_4 to reproduce the calculated energies reported in Table 2.

Table 2. Relative Energies of the Magnetic Phases Described above with Respect to the FM phase (in cm^{-1}) for the UHF and B3LYP Methods and the Corresponding Energy Expression in Terms of J_1, J_2, J_3, and J_4 Using Equation 2a

phase	UHF	B3LYP	energy expression[a]
E(FM-FM)	0.0	0.0	0
E(FM-AF)	−34.56	−220.60	$8J_3 + 16J_4$
E(AF-FM)	−59.69	−231.22	$16J_1 + 16J_4$
E(AF-AF)	−75.41	−37.26	$16J_1 + 8J_3$
E(ABBA)	−17.82	−111.34	$4J_3 + 8J_4$
E(FAFA)	−42.86	−123.16	$8J_1 + 4J_3 + 8J_4$
E(AAAB)	−17.78	−111.01	$4J_3 + 8J_4$
E(AFM1)	−31.27	−130.27	$8J_1 + 4J_2 + 8J_4$
E(AFM2)	−32.63	−143.68	$8J_1 + 8J_2 + 8J_4$

[a] Using eq 2b simply introduces a factor 2 for all the coefficients. All the energy differences reported refer to magnetic cells including 16 O_3^- units.

Table 3. Estimated Values for J_1, J_2, J_3, and J_4 (in cm^{-1}) using UHF and B3LYP Methods and the Set of Equations Described in Table 2

	UHF eq 2a (2b)	B3LYP eq 2b (2a)
J_1	−3.14 (−1.57)	−0.74 (−1.50)
J_2	−0.34 (−0.17)	−1.76 (−3.52)
J_3	−3.18 (−1.59)	−0.85 (−1.70)
J_4	−0.60 (−0.30)	−6.59 (−12.98)

In all cases, as expected from the experimentally determined magnetic properties, the calculated coupling constants are weak and showing a significant dependence on the method. For both methods, antiferromagnetic interactions are found to be dominant, although the predicted magnetic behavior is different. The UHF calculations predict the system to behave as a 3D antiferromagnet built from antiferromagnetic *ab* layers (J_1) coupled antiferromagnetically along the *c* axis (J_3), with similar values for effective magnetic coupling along all three crystallographic axes. The B3LYP method, which in general has been found to give a better description of the magnetic structure than the UHF one, predicts a quite distinct magnetic behavior: the relative values of the coupling constants indicate a significant one-dimensional (1D) character with complex antiferromagnetic chains along the *c* axis (dominated by J_4) and a weaker antiferromagnetic coupling between neighboring chains (J_1 and J_2). This behavior is consistent with the experimental susceptibility curve determined by Lueken et al.[21] in which a broad maximum at 20 K is followed by a minimum at 6 K, a feature that is observed in cases in which the paramagnetic centers order first in antiferromagnetic chains or layers that order themselves at lower temperatures to give a weaker 3D magnetic structure.

The interpretation of the experimental behavior given by Lueken et al.[21] based on the shortest distances

between O_3^- units is, however, different from what we find in our B3LYP calculations. While the maximum in susceptibility is assigned by Lueken et al.[21] to the formation of antiferromagnetic layers parallel to the *ab* planes, our calculations suggest that the low dimensional magnetic arrangement is due to antiferromagnetic coupling in chains along the *c* direction, that is, perpendicular to those planes. It is worth mentioning that the magnetic coupling is dominated by overlap between the magnetic orbitals of neighbor magnetic centers which is not always associated to the shortest distances. In the case of KO_3, the π magnetic orbitals of O_3^- units are delocalized along the *c* axis favoring couplings at longer distances in this direction than within *ab* planes. As a final comment, the different description of the dominant magnetic couplings provided by UHF and B3LYP can be related to the different spin distribution observed for the magnetic O_3^- units by the different methods. Hence, a strong localization of spin density on O(1) enhances the overlap with neighboring O_3^- units along J_1 and J_3 (shortest O(1)···O(1) and O(1)···O(2) distances) whereas large delocalization on O(2) favors interactions along J_2 and J_4 (shortest O(2)···O(2) distances) involving large lobes of the π system.

Regarding the maximum in the susceptibility at $T = 20$ K observed for KO_3,[21] the *J* value is expected to be close to -20 K (-14 cm^{-1}) for a magnetic system consisting in simple dimers or chains. However, the calculations suggest that the system exhibits a rather complex magnetic structure with a dominant 1D character. Hence, the average interaction derived from the Curie−Weiss constant seems more adequate to estimate its value. The high temperature part of the experimental curve follows the Curie−Weiss (CW) law[3,4] as

$$\chi_p = \frac{C}{T - \Theta} \tag{3}$$

where

$$\Theta = \frac{zJ_{CW}S(S+1)}{3k} \tag{4}$$

where J_{CW} may be seen as a parameter controlling the interaction between a given $S = 1/2$ magnetic center with its *z* nearest neighbor sites, and Θ is the so-called Weiss constant which in this compound is found[21] to be $\Theta = -34$ K indicating AFM interactions. From the Weiss parameter it is possible to infer the J_{CW} value, although this requires the a priori assumption of the number of nearest neighbors. For $z = 1$ (dimers) eq 4 yields $J_{CW} = -94.6$ cm^{-1}; for $z = 2$ (chains) $J_{CW} = -47.3$ cm^{-1}; for $z = 4$ (planes) $J_{CW} = -23.6$ cm^{-1}; for $z = 6$ (3D) $J_{CW} = -15.8$ cm^{-1}. Although the J_i values obtained using the B3LYP method are somewhat smaller than these estimated J_{CW} values, the magnitudes of J_{CW} corresponding to either the 1D or the two-dimensional (2D) models are in qualitative agreement with the picture of the magnetic structure dominated by J_2 and J_4 provided by the B3LYP results. This fact and the reliability of the B3LYP approach in describing other magnetic systems provide enough confidence to consider that the present B3LYP calculations consistently describe the electronic structure and magnetic properties of KO_3 and similar open shell materials.

Conclusions

Ab inito electronic structure calculations are able nowadays to give reliable information on the exchange coupling behavior in complex systems like KO_3 where the unpaired electrons cannot be assigned to single atoms in the structure. Our calculations show that KO_3 is a strongly ionic compound with paramagnetic O_3^- anions. For all methods, the DOS show clearly that the system behaves as an insulator with a gap of ~3.0 eV, as suggested by the (spin unrestricted) B3LYP method, and with states around the insulating gap arising mainly from the π orbitals of the O_3^- units and with a negligible participation of potassium orbitals in the bands around the band gap. Although the gross features of the DOS and its projections are very similar for the four methods used to obtain the electronic structure of KO_3, the details depend on the functional. The calculated magnetic structure for KO_3 is in agreement with the available experimental data explaining the departure from the Curie−Weiss behavior for this compound. Considering the calculated magnetic coupling constants between neighboring O_3^- anions, our calculations suggest that the complex low temperature magnetic behavior may be attributed to antiferromagnetically coupled complex $\cdots O_3^- \cdots O_3^- \cdots$ chains along the *c* direction that couple themselves also antiferromagnetically at even lower temperatures. This result provides a nice example of a low dimensional magnetic system formed by magnetic centers with $S = 1/2$ spin which are molecular species rather than simple ions which also dominate the conducting properties of the system. Finally, from the present results it is expected that ozonides including paramagnetic transition metal cations would exhibit very interesting magnetic properties, and synthesis of this kind of new materials is encouraged.

Acknowledgment. Financial support from the Spanish *Ministerio de Ciencia e Innovación*, projects CTQ2008-06670-C02-02/BQU and FIS2008-02238/FIS and, in part, from the *Generalitat de Catalunya* projects 2005SGR-00036 and 2005SGR-000697 is fully acknowledged. Miquel Llunell gratefully acknowledges the *Ramón y Cajal Program* for a postdoctoral position.